

INVESTIGATING IMPACT MINERALOGY THROUGH LASER-HEATED RAPID-DECOMPRESSION

OF ENSTATITE M. Anae¹, D. Darnulc¹, M. Harms³, S. Lobanov³, A. Pakhomova⁴, R. Husband⁴, H. P. Liermann⁴, and L. Ehm^{1,2}, ¹Department of Geosciences, Stony Brook University, Stony Brook, NY 11794, USA, ²Mineral Physics Institute, Stony Brook University, Stony Brook, NY 11794, USA, ³Deutsches GeoForschungsZentrum GFZ, D-14473 Potsdam, Germany, ⁴Deutsches Elektronen-Synchrotron, D-22607 Hamburg, Germany

Introduction: High-velocity impacts contribute to the formation and differentiation of planetary bodies and the phase conditions of these events can offer insight into the mineralogy of planetary interiors. The extreme pressure and temperature conditions of an impact event leave a signature in target rock and ejecta. In meteorites and impactites, the impact conditions are generally constrained on the mineralogical scale based on the presence of high pressure polymorphs of major rock forming minerals and/or changes in the microstructure of minerals [1,2]. Recently, high pressure polymorphs of MgSiO_3 , namely bridgmanite and the tetragonal MgSiO_3 garnet phase, have been identified in the Tenham L6 chondrite meteorite [3,4]. The equilibrium phase diagram of MgSiO_3 has been used to estimate the peak pressure and temperature conditions during the impact event. However, Sims et al have shown that for plagioclase, the use of the equilibrium phase diagram to constrain the peak pressure conditions in impacts is problematic, since the location of phase boundaries in p,T space are path dependent [5]. Additionally, the investigation of the mineral phase assemblage in meteorites occurs after decompression and cooling as well as subsequent weathering and alteration, and do not necessarily reflect the phases formed during impact [1].

We have conducted *in situ* high temperature rapid-decompression experiments of MgSiO_3 to provide additional constraints on the pressure-temperature-time pathways that lead to the formation of high pressure polymorphs of MgSiO_3 in meteorites.

Methods: Laser-heated rapid decompression experiments with simultaneous *in situ* time-resolved X-ray diffraction measurements were conducted at the Extreme Conditions Beamline (P02.2) at the PETRA III synchrotron using membrane driven diamond anvil cells (DAC) [6]. The sample was a synthetic mixture of clino and ortho-enstatite (6 wt% clino and 93 wt% ortho-enstatite), ground in an agate mortar and mixed with about 6 wt% platinum powder. Platinum served as a coupler for the laser heating and as internal pressure standard [7]. The sample was loaded into the DAC using a stainless steel gasket with a hole diameter of 100 μm and a pre-indented thickness of 50 μm . Time-resolved synchrotron powder diffraction data were collected with a time resolution of 1 s per diffraction

image. We conducted a total of nine decompression runs, with two different decompression rates each for three different temperatures. The temperatures of the runs were determined using spectral pyrometry with a time resolution of 5 s and the spectra were fitted with the program T-Rax using a Planck radiation function with a grey body approximation [8]. The 2D diffraction images were converted to conventional 1D diffraction patterns and quantitatively analyzed using the program DIOPTAS [9]. Diffraction patterns were analyzed using the Rietveld method. The pressure for each diffraction pattern were determined from the unit cell volume of the internal Pt pressure standard using the p,T equation of state by Dorogokupets and Dewaele [7].

We examined selected recovered samples with a Zeiss LEO1550 SFEG-SEM. Gold-coated samples were imaged with Robinson Backscatter (RBSD) and Secondary Electron Detectors (SED) at 20 kV and 2.5 kV respectively. The microstructure and grain size distribution was determined using Fiji ImageJ [10].

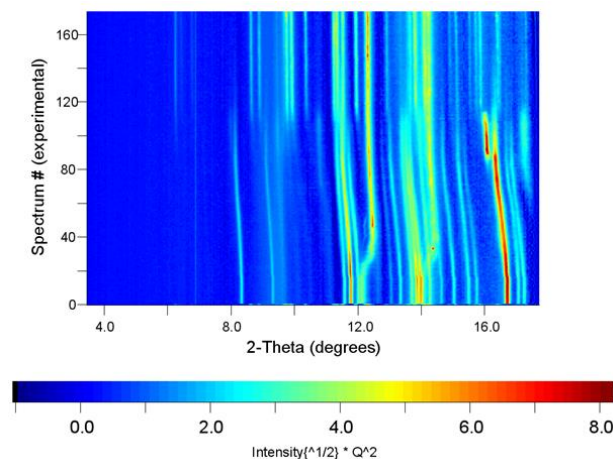


Figure 1. Contour plot showing the evolution of diffraction patterns with time (spectrum# is equivalent to time in seconds) at high temperature ($\sim 1700(100)$ K) with a rapid decompression rate of 0.15 GPa/s. Phase transitions are clearly visible in the plot by the appearance and disappearance of diffraction signals.

Results & Discussion: Enstatite underwent ambient temperature adiabatic compression into the bridgmanite stability field, followed by heating for a 1 s interval before the start of the decompression ramp. Fig. 1 shows

the evolution of diffraction patterns at quasi-isothermal conditions for our representative run. We see the near instantaneous formation of bridgmanite at the introduction of temperature. Bridgmanite persists significantly passed the equilibrium phase boundary, into phase regimes as low as high-P clinoenstatite. During decompression, each back transformation is notably shifted, indicating a metastable extension of the stability of the high pressure phases to lower pressures. All phases or decompositions of the equilibrium phase diagram are observed, except for the formation of tetragonal garnet. At the lowest pressures, bridgmanite is regularly back transformed to ortho-enstatite and does not persist to ambient pressures. Diffraction patterns at the end of the run, and after quenching, reveal no high pressure phases; only the low pressure phases and decomposition products are present. We see small variations in grain size and texture between runs. Grain sizes have an average of $\sim 1.3 \mu\text{m}$ across all SEM imaged samples. The textures are either equant or acicular, with needles occurring at higher temperatures (Fig.2), and becoming more rare with less heating.

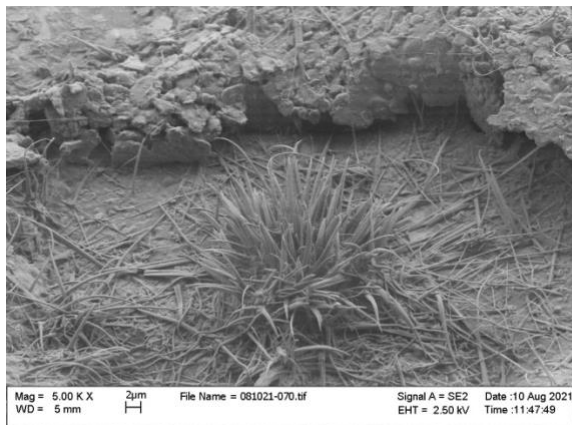


Figure 2: SEM image of the recovered sample after heating to $\sim 1800 \text{ K}$ and decompression at 0.1 GPa/s . The samples show acicular grain assemblage at the center of the sample, measuring $15.7 \mu\text{m}$ across. Sparse needles occur on other samples indicating a growth of the low pressure phases along the pressure and temperature gradient in the cell.

The absence of the tetragonal garnet phase is of particular interest since this phase has been observed in multiple chondrites, including the Tenham meteorite [3,4]. We suspect our experiment has not reached the critical timescale required to nucleate garnet. Depending on the decompression rate, the stability field of garnet is traversed in 1-5 s, indicating more time is necessary to form this phase. The pressure of impact events is characterized with a rapid, near vertical

increase, and a plateau of peak pressure before decompression. The pressure duration of impacts is controlled by the size of the parent body and velocity of impact. We speculate that tetragonal garnet forms during impacts where the peak pressure plateau is relatively long, exceeding the conditions of this experiment, and thus increasing the time spent in the stability field of tetragonal garnet allowing the phase to nucleate.

The conditions necessary to retain bridgmanite at ambient pressure in the Tenham meteorite are also uncertain. Even though we see a persistence of bridgmanite beyond its stability field in this work, at the end of each run it transforms back to orthoenstatite. We speculate residual compression strain of shock events may prevent the back transformation from bridgmanite to subsequent phases. The remaining compression strain could stabilize the high pressure phase and explain the observation of bridgmanite at ambient conditions.

While DAC experiments are unable to recreate the shockwaves of impacts, *in situ* probes coupled with dynamic experimentation are highly valuable to characterize phase transformations in real time and provide firm experimental constraints for the interpretation of impactites.

Acknowledgements: The research was supported by NASA through the SSW program under grant 80NSSC17K0765. MA is grateful for the support of the W. Burkhardt Turner Fellowship. DD acknowledges the support by a travel award from the JPSI at SBU. We would like to thank D. Lindsley for providing the enstatite sample. We acknowledge DESY (Hamburg, Germany), a member of the Helmholtz Association HGF, for providing the experimental facilities. Parts of this research were carried out at the P02.2 Extreme Conditions Beamline at PETRA III.

References:

- [1] Fritz J. et al. (2017) *Meteorit. Planet. Sci.* 52, 1212-1232. [2] Stoeffler D. et al. (1991) *Geochim. Cosmochim. Acta*, 55, 3845-3867. [3] Tschauner O. et al. (2014) *Science*, 346, 1100-1102. [4] Tomioka N. et al. (2016) *Science Advances*, 2, 10501725. [5] Sims M. et al. (2019), *EPSL*, 507, 166-174. [6] Liermann H. P. et al. (2015), *JSR*, 22, 908-924. [7] Dorogokupets P. I. and Dewaele A. (2007) *High Press. Res.*, 27, 431-446. [8] Holtgreve N. et al. (2019), *High Press Res*, 39, 457-470. [9] Prescher, C. and Prakapenka, V.B. (2015) *High Press. Res.*, 35, 223-230. [10] Schindelin, J. et al. (2012), *Nature Methods*, 9, 676-682.